Proceedings of the 31st Conference
on Decision and Control
Tucson, Arizona • December 1992

COORDINATING LOCOMOTION AND MANIPULATION OF A MOBILE MANIPULATOR

Yoshio Yamamoto and Xiaoping Yun
General Robotics and Active Sensory Perception (GRASP) Laboratory
University of Pennsylvania
3401 Walnut Street, Room 301C
Philadelphia, PA 19104-6228

ABSTRACT

A mobile manipulator in this study is a manipulator mounted on a mobile platform. Assuming the end point of the manipulator is guided, *e.g.*, by a human operator to follow an arbitrary trajectory, it is desirable that the mobile platform is able to move as to position the manipulator in certain preferred configurations. Since the motion of the manipulator is unknown *a priori*, the platform has to use the measured joint position information of the manipulator for motion planning. This paper presents a planning and control algorithm for the platform so that the manipulator is always positioned at the preferred configurations measured by its manipulability. Simulation results are presented to illustrate the efficacy of the algorithm. Also the algorithm is implemented and verified on a real mobile manipulator system. The use of the resulting algorithm in a number of applications is also discussed.

1 Introduction

When a human writes across a board, he positions his arm in a comfortable writing configuration by moving his body rather than reaching out his arm. Also when humans transport a large and/or heavy object coorperatively, they tend to prefer certain configurations depending on various factors, *e.g.*, the shape and the weight of the object, the transportation velocity, the number of people involved in a task, and so on. Therefore when a mobile manipulator performs a manipulation task, it is desirable to bring the manipulator into certain preferred configurations by appropriately planning the motion of the mobile platform. If the trajectory of the manipulator end point in a fixed coordinate system (world coordinate system) is known *a priori*, then the motion of the mobile platform can be planned accordingly. However, if the motion of the manipulator end point is unknown *a priori*, *e.g.*, driven by a visual sensor or guided by a human operator, then the path planning has to be made locally and in real time rather than globally and off-line. This paper presents a planning and control algorithm for the platform in the latter case, which takes the measured joint displacement of the manipulator as the input for motion planning, and controls the platform in order to bring the manipulator into a preferred operating region. While this region can be selected based on any meaningful criterion, the manipulability measure [1] is utilized in this study. By using this algorithm, the mobile platform will be able to "understand the intention of its manipulator and respond accordingly."

This control algorithm has a number of immidiate applications. First, a human operator can easily move around the mobile manipulator by "dragging" the end point of the manipulator while the manipulator is in the free mode (compensating the gravity only). Second, if the manipulator is force-controlled, the mobile manipulator will be able to push against and follow an external moving surface. Third, when two mobile manipulators transport a large object with one being the master and the other being slave, this algorithm can be used to control the slave mobile manipulator to support the object and follow the motion of the master, resulting in a cooperative control algorithm for two mobile manipulators.

Although there has been a vast amount of research effort on mobile platforms (commonly referred to as mobile robots) in the literature, the study on mobile manipulators is very limited. Joshi and Desrochers considered a two link manipulator on a moving platform subject to random disturbances in its orientation [2]. Wien studied dynamic coupling between a planar vehicle and a one-link manipulator on the vehicle [3]. Dubowsky, Gu, and Deck derived the dynamic equations of a fully spatial mobile manipulator with link flexibility [4]. Recently, Hootsmans proposed a mobile manipulator control algorithm (the Mobile Manipulator Jacobian Transpose Algorithm) for a dynamically coupled mobile manipulator [5]. He showed that with the algorithm the manipulator could successfully compensate a trajectory error caused by vehicle's passive suspension with the help of limited sensory information from mobile vehicle.

What makes the coordination problem of locomotion and manipulation a difficult one is twofold. First, a manipulator and a mobile platform, in general, have different dynamic characteristics, namely, a mobile platform has slower dynamic response than a manipulator. Second, a wheeled mobile platform is subject to nonholonomic constraints while a manipulator is usually unconstrained. These two issues must be taken into consideration in developing a planning and control algorithm.

Dynamic modeling of mechanical systems with nonholonomic constraints is richly documented by work ranging from Neimark and Fufaev's comprehensive book [6] to more recent developments (see for example, [7]). However, the literature on control properties of such systems is sparse [8]. The interest in control of nonholonomic systems has been stimulated by the recent research in robotics. The dynamics of a wheeled mobile robot is nonholonomic [9], and so is a multi-arm system manipulating an object through the whole arm manipulation [10].

Bloch and McClamroch [8] first demonstrated that a nonholonomic system cannot be feedback stabilized to a single equilibrium point by a smooth feedback. In a follow-up paper [11], they showed that the system is small-time locally controllable. Campion *et al* [12] showed that the system is controllable regardless of the structure of nonholonomic constraints. Motion planning of mobile robots has been an active topic in robotics in the past several years [13, 14, 9, 15, 16]. Nevertheless, much less is known about the dynamic control of mobile robots with nonholonomic constraints and the developments in this area are very recent [17, 18, 19].

In this paper, we first present the theoretic formulation of a general nonholonomic system. Next we apply the formulation to the specific mobile platform used for the experiments in order to derive the dynamic equations. Then we describe the path planning algorithm and show the simulation and experimental results followed by concluding remark.

2 Nonholonomic Systems

2.1 Dynamic Equations of Motion

Consider a mechanical system with n generalized coordinates q subject to m bilateral constraints whose equations of motion are described by

$$M(q)\ddot{q} + V(q,\dot{q}) = E(q)\tau - A^T(q)\lambda \tag{1}$$

where $M(q)$ is the $n \times n$ inertia matrix, $V(q,\dot{q})$ is the vector of position and velocity dependent forces, $E(q)$ is the $n \times r$ input transformation matrix[1], τ is the r-dimensional input vector, $A(q)$ is the $m \times n$ Jacobian matrix, and λ is the vector of constraint forces. The m constraint equations of the mechanical system can be written in the form

$$C(q,\dot{q}) = 0 \tag{2}$$

If a constraint equation is in the form $C_i(q) = 0$, or can be integrated into this form, it is a holonomic constraint. Otherwise it is a kinematic (not geometric) constraint and is termed nonholonomic.

We assume that we have k holonomic and $m - k$ nonholonomic independent constraints, all of which can be written in the form of

$$A(q)\dot{q} = 0 \tag{3}$$

[1] $E(q)$ is an identity matrix in most cases. However, if the generalized coordinates are chosen to be some variables other than the joint variables, or if there are passive joints without actuators, it is not an identity matrix.

Let $s_1(q), \cdots, s_{n-m}(q)$ be a set of smooth and linearly independent vector fields in the null space of $A(q)$, *i.e.*,

$$A(q)s_i(q) = 0 \qquad i = 1, \ldots, n-m.$$

Let $S(q)$ be the full rank matrix made up of these vectors

$$S(q) = [s_1(q) \quad \cdots \quad s_{n-m}(q)] \tag{4}$$

and let Δ be the distribution spanned by these vector fields

$$\Delta = span\{s_1(q), \quad \cdots, \quad s_{n-m}(q)\}$$

It follows that $\dot{q} \in \Delta$. Δ may or may not be involutive. For that reason, we let Δ^* be the smallest involutive distribution containing Δ. It is clear that $dim(\Delta) \leq dim(\Delta^*) = k$. There are three possible cases (as observed by Campion, *et al.* in [12]). First, if $k = m$, that is, all the constraints are holonomic, then Δ is involutive itself. Second, if $k = 0$, that is, all the constraints are nonholonomic, then Δ^* spans the entire space. Finally, if $0 < k < m$, the k constraints are integrable and k components of the generalized coordinates may be eliminated from the motion equations. In this case, $dim(\Delta^*) = n - k$.

2.2 State Space Representation

We now consider the mechanical system given by (1) and (3). Since the constrained velocity is always in the null space of $A(q)$, it is possible to define $n - m$ velocities $\nu(t) = [\nu_1 \quad \nu_2 \cdots \nu_{n-m}]$ such that

$$\dot{q} = S(q)\nu(t) \tag{5}$$

These velocities need not be integrable.

Differentiating Equation (5), substituting the expression for $\ddot{q}$ into (1), and premultiplying by S^T, we have

$$S^T(MS\dot{\nu}(t) + M\dot{S}\nu(t) + V) = S^T E\tau \tag{6}$$

by noting that

$$A(q)\dot{q} = 0. \tag{7}$$

Using the state space variable $x = [q^T \quad \nu^T]^T$, we have

$$\dot{x} = \begin{bmatrix} S\nu \\ f_2 \end{bmatrix} + \begin{bmatrix} 0 \\ (S^TMS)^{-1}S^TE \end{bmatrix}\tau \tag{8}$$

where $f_2 = (S^TMS)^{-1}(-S^TM\dot{S}\nu - S^TV)$. Assuming that the number of actuator inputs is greater or equal to the number of the degrees of freedom of the mechanical system ($r \geq n - m$), and $(S^TMS)^{-1}S^TE$ has rank $n - m$, we may apply the following nonlinear feedback

$$\tau = ((S^TMS)^{-1}S^TE)^+(u - f_2) \tag{9}$$

where the superscript + denotes the generalized matrix inverse. The state equation simplifies to the form

$$\dot{x} = f(x) + g(x)u \tag{10}$$

where $f(x) = \begin{bmatrix} S(q)\nu \\ 0 \end{bmatrix}$, $g(x) = \begin{bmatrix} 0 \\ I \end{bmatrix}$.

2.3 Control Properties

The following two properties of the system (10) have been established in [12, 8, 11] for the special case in which *all* constraints are nonholonomic.

Theorem 1 *The nonholonomic system (10) is controllable.*

Theorem 2 *The equilibrium point $x = 0$ of the nonholonomic system (10) can be made Lagrange stable, but can not be made asymptotically stable by a smooth state feedback.*

In the rest of this section, we discuss the more general case in which Equation (3) consists of both holonomic and nonholonomic constraints.

Theorem 3 *System (10) is not input-state linearizable by a state feedback if at least one of the constraints is nonholonomic.*

Proof: The system has to satisfy two conditions for input-state linealization: the strong accessibility condition and the involutivity condition [20]. It is shown below that the involutivity condition is not satisfied.

Define a sequence of distributions

$$D_j = span\{L_f^i g \mid i = 0, 1, \ldots, j-1\}, \quad j = 1, 2, \ldots$$

Then the involutivity condition requires that the distributions D_1, D_2, $\ldots$, D_{2n-m} are all involutive. Note that the dimension of the state variable is $2n - m$. $D_1 = span\{g\}$ is involutive since g is constant. Next we compute

$$L_f g = [f, g] = \frac{\partial g}{\partial x}f - \frac{\partial f}{\partial x}g = -\begin{bmatrix} S(q) \\ 0 \end{bmatrix}$$

Since the distribution Δ spanned by the columns of $S(q)$ is not involutive, the distribution $D_2 = span\{g, L_f g\}$ is not involutive. Therefore, the system is not input-state linearizable. □

Although a system with nonholonomic constraints is not input-state linearizable, it is input-output linearizable if a proper set of output equations are chosen. Consider the position control of the system, *i.e.*, the output equations are functions of position state variable q only. Since the number of the degrees of freedom of the system is instantaneously $n - m$, we may have at most $n - m$ independent position outputs equations.

$$y = h(q) = [h_1(q) \quad \cdots \quad h_{n-m}(q)] \tag{11}$$

The necessary and sufficient condition for input-output linearization is that the decoupling matrix has full rank [20]. With the output equation (11), the decoupling matrix $\Phi(x)$ for the system is the $(n - m) \times (n - m)$ matrix

$$\Phi(q) = J_h(q)S(q) \tag{12}$$

where $J_h = \frac{\partial h}{\partial q}$ is the $(n-m)\times n$ Jacobian matrix. $\Phi(x)$ is nonsingular if the rows of J_h are independent of the rows of $A(q)$.

To characterize the zero dynamics and achieve input-output linearization, we introduce a new state space variable z defined as follows

$$z = T(x) = \begin{bmatrix} z_1 \\ z_2 \\ z_3 \end{bmatrix} = \begin{bmatrix} h(q) \\ L_f h(q) \\ \tilde{h}(q) \end{bmatrix} = \begin{bmatrix} h(q) \\ \Phi(q)\nu \\ \tilde{h}(q) \end{bmatrix} \tag{13}$$

where $\tilde{h}(q)$ is an m-dimensional function such that $[J_h^T \quad J_{\tilde{h}}^T]$ has full rank. It is easy to verify that $T(x)$ is indeed a diffeomorphism and thus a valid state space transformation. The system under the new state variable z is characterized by

$$\dot{z}_1 = \frac{\partial h}{\partial q}\dot{q} = z_2 \tag{14}$$

$$\dot{z}_2 = \dot{\Phi}(q)\nu + \Phi(q)u \tag{15}$$

$$\dot{z}_3 = J_{\tilde{h}}S\nu = J_{\tilde{h}}S(J_hS)^{-1}z_2 \tag{16}$$

Utilizing the following state feedback

$$u = \Phi^{-1}(q)(v - \dot{\Phi}(q)\nu) \tag{17}$$

we achieve input-output linearization as well as input-output decoupling by noting the observable part of the system

$$\dot{z}_1 = z_2 \qquad \dot{z}_2 = v \qquad y = z_1$$

The unobservable zero dynamics of the system is (obtained by substituting $z_1 = 0$ and $z_2 = 0$)

$$\dot{z}_3 = 0 \tag{18}$$

which is clearly Lagrange stable but not asymptotically stable.

3 Mobile Platform

3.1 Constraint Equations

In this subsection, we derive the constraint equations for a LABMATE[2] mobile platform. The platform has two driving wheels (the center ones) and four passive supporting wheels (the corner ones). The two driving wheels are independently driven by two DC motors, respectively. The following notations will be used in the derivation of the constraint equations and dynamic equations (see Figure 1).

[2]LABMATE is a trademark of Transitions Research Corporation.

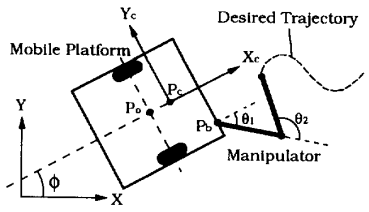

Figure 1: Schematic of the mobile manipulator.

P_o: the intersection of the axis of symmetry with the driving wheel axis;
P_c: the center of mass of the platform;
P_b: the location of the manipulator on the platform;
P_r: the reference point to be followed by the mobile platform;
d: the distance from P_o to P_c;
b: the distance between the driving wheels and the axis of symmetry;
r: the radius of each driving wheel;
m_c: the mass of the platform without the driving wheels and the rotors of the DC motors;
m_w: the mass of each driving wheel plus the rotor of its motor;
I_c: the moment of inertia of the platform without the driving wheels and the rotors of the motors about a vertical axis through P_o;
I_w: the moment of inertia of each wheel and the motor rotor about the wheel axis;
I_m: the moment of inertia of each wheel and the motor rotor about a wheel diameter.

There are three constraints. The first one is that the platform must move in the direction of the axis of symmetry, *i.e.*,

$$\dot{y}_c \cos\phi - \dot{x}_c \sin\phi - d\dot{\phi} = 0 \tag{19}$$

where (x_c, y_c) is the coordinates of the center of mass P_c in the world coordinate system, and the ϕ is the heading angle of the platform measured from the X-axis of the world coordinates. The other two constraints are the rolling constraints, *i.e.*, the driving wheels do not slip.

$$\dot{x}_c \cos\phi + \dot{y}_c \sin\phi + b\dot{\phi} = r\dot{\theta}_r \tag{20}$$

$$\dot{x}_c \cos\phi + \dot{y}_c \sin\phi - b\dot{\phi} = r\dot{\theta}_l \tag{21}$$

where θ_r and θ_l are the angular displacement of the right and left wheels, respectively.

Let $q = (x_c, y_c, \phi, \theta_r, \theta_l)$, the three constraints can be written in the form of

$$A(q)\dot{q} = 0$$

where

$$A(q) = \begin{bmatrix} -\sin\phi & \cos\phi & -d & 0 & 0 \\ -\cos\phi & -\sin\phi & -b & r & 0 \\ -\cos\phi & -\sin\phi & b & 0 & r \end{bmatrix} \tag{22}$$

It is straightforward to verify that the following matrix

$$S(q) = [s_1(q),\ s_2(q)] = \begin{bmatrix} c(b\cos\phi - d\sin\phi) & c(b\cos\phi + d\sin\phi) \\ c(b\sin\phi + d\cos\phi) & c(b\sin\phi - d\cos\phi) \\ c & -c \\ 1 & 0 \\ 0 & 1 \end{bmatrix}$$

satisfies $A(q)S(q) = 0$, where the constant $c = \frac{r}{2b}$. Computing the Lie bracket of $s_1(q)$ and $s_2(q)$ we obtain

$$s_3(q) = [s_1(q),\ s_2(q)] = \begin{bmatrix} -rc\sin\phi \\ rc\cos\phi \\ 0 \\ 0 \\ 0 \end{bmatrix}$$

which is not in the distribution Δ spanned by $s_1(q)$ and $s_2(q)$. Therefore, at least one of the constraints is nonholonomic. We continue to compute the Lie bracket of $s_1(q)$ and $s_3(q)$

$$s_4(q) = [s_1(q),\ s_3(q)] = \begin{bmatrix} -rc^2\cos\phi \\ -rc^2\sin\phi \\ 0 \\ 0 \\ 0 \end{bmatrix}$$

which is linearly independent of $s_1(q)$, $s_2(q)$, and $s_3(q)$. However, the distribution spanned by $s_1(q)$, $s_2(q)$, $s_3(q)$ and $s_4(q)$ is involutive. Therefore, we have

$$\Delta^* = span\{s_1(q),\ s_2(q),\ s_3(q),\ s_4(q)\} \tag{23}$$

It follows that, among the three constraints, two of them are nonholonomic and the third one is holonomic. To obtain the holonomic constraint, we subtract Equation (21) from Equation (20).

$$2b\dot{\phi} = r(\dot{\theta}_r - \dot{\theta}_l) \tag{24}$$

Integrating the above equation and properly choosing the initial condition of θ_r and θ_l, we have

$$\phi = c(\theta_r - \theta_l) \tag{25}$$

which is clearly a holonomic constraint equation.

3.2 Dynamic Equations

We now derive the dynamic equation for the mobile platform. The Lagrange equations of motion of the platform with the Lagrange multipliers λ_1, λ_2, and λ_3 are given by

$$m\ddot{x}_c - m_c d(\ddot{\phi}\sin\phi + \dot{\phi}^2\cos\phi) - \lambda_1\sin\phi - (\lambda_2 + \lambda_3)\cos\phi = 0 \tag{26}$$

$$m\ddot{y}_c + m_c d(\ddot{\phi}\cos\phi - \dot{\phi}^2\sin\phi) + \lambda_1\cos\phi - (\lambda_2 + \lambda_3)\sin\phi = 0 \tag{27}$$

$$-m_c d(\ddot{x}_c\sin\phi - \ddot{y}_c\cos\phi) + I\ddot{\phi} - d\lambda_1 + b(\lambda_3 - \lambda_2) = 0 \tag{28}$$

$$I_w\ddot{\theta}_r + \lambda_2 r = \tau_r \tag{29}$$

$$I_w\ddot{\theta}_l + \lambda_3 r = \tau_l \tag{30}$$

where

$$\begin{aligned} m &= m_c + 2m_w \\ I &= I_c + 2m_w(d^2 + b^2) + 2I_m \end{aligned}$$

and τ_r and τ_l are the torques acting on the wheel axis generated by the right and left motors respectively. These five equations of motion can easily be written in the form of Equation (1). The matrix $A(q)$ has been defined in Equation (22). The matrices $M(q)$, $V(q,\dot{q})$, and $E(q)$ are given by

$$M(q) = \begin{bmatrix} m & 0 & -m_c d\sin\phi & 0 & 0 \\ 0 & m & m_c d\cos\phi & 0 & 0 \\ -m_c d\sin\phi & m_c d\cos\phi & I & 0 & 0 \\ 0 & 0 & 0 & I_w & 0 \\ 0 & 0 & 0 & 0 & I_w \end{bmatrix}$$

$$V(q,\dot{q}) = \begin{bmatrix} -m_c d\dot{\phi}^2\cos\phi \\ -m_c d\dot{\phi}^2\sin\phi \\ 0 \\ 0 \\ 0 \end{bmatrix}, \qquad E(q) = \begin{bmatrix} 0 & 0 \\ 0 & 0 \\ 0 & 0 \\ 1 & 0 \\ 0 & 1 \end{bmatrix}$$

In this case, owing to the choice of $S(q)$ matrix, we have

$$\nu = \begin{bmatrix} \nu_1 \\ \nu_2 \end{bmatrix} = \begin{bmatrix} \dot{\theta}_r \\ \dot{\theta}_l \end{bmatrix}$$

The state variable is then

$$x = [x_c \quad y_c \quad \phi \quad \theta_r \quad \theta_l \quad \dot{\theta}_r \quad \dot{\theta}_l]$$

Using this state variable, the dynamics of the mobile platform can be represented in the state space form, Equation (8).

3.3 Output Equations

While the state equation of a dynamic system is uniquely, modulo its representation, determined by its dynamic characteristics, the output equation is chosen in such a way that the tasks to be performed by the dynamic system can be *conveniently specified* and that the controller design can be *easily accomplished*. For example, if a 6-DOF robot manipulator is to perform pick-and-place or trajectory tracking tasks, the six-dimensional joint position vector or the 6-dimensional Cartesian position and orientation vector is normally chosen as the output equation. In this section, we present the output equation for the mobile platform and discuss its properties.

It is convenient to define a platform coordinate frame X_c-Y_c at the center of mass of at the mobile platform, with X_c in the forward direction of the platform. We may choose an arbitrary point P_r with respect to the platform coordinate frame X_c-Y_c as a reference point.

The mobile platform is to be controlled so that the reference point follows a desired trajectory. Let the reference point be denoted by (x_r^c, y_r^c) in the platform frame X_c-Y_c. Then the world coordinates (x_r, y_r) of the reference point are given by

$$x_r = x_c + x_r^c \cos\phi - y_r^c \sin\phi \quad (31)$$
$$y_r = y_c + x_r^c \sin\phi + y_r^c \cos\phi \quad (32)$$

The selection of the reference point for the purpose of coordinating locomotion and manipulation is discussed in the following section. Having chosen the reference point, x_r^c and y_r^c are constant. By taking the coordinates of the reference point to be the output equation

$$y = h(q) = [x_r \quad y_r]^T \quad (33)$$

we have a trajectory tracking problem studied in [17, 18]. The corresponding decoupling matrix for this output is

$$\Phi(q) = J_h(q)S(q) = \begin{bmatrix} \Phi_{11} & \Phi_{12} \\ \Phi_{21} & \Phi_{22} \end{bmatrix} \quad (34)$$

where

$$\Phi_{11} = c((b - y_r^c)\cos\phi - (d + x_r^c)\sin\phi) \quad (35)$$
$$\Phi_{12} = c((b + y_r^c)\cos\phi + (d + x_r^c)\sin\phi) \quad (36)$$
$$\Phi_{21} = c((b - y_r^c)\sin\phi + (d + x_r^c)\cos\phi) \quad (37)$$
$$\Phi_{21} = c((b + y_r^c)\sin\phi - (d + x_r^c)\cos\phi) \quad (38)$$

Since the determinant of the decoupling matrix is $\det(\Phi(q)) = -\frac{r^2(d+x_r^c)}{2b}$, it is singular if and only if $x_r^c = -d$, that is, the point P_r is located on the wheel axis. Therefore, trajectory tracking of a point on the wheel axis including P_o is not possible as pointed out in [18]. This is clearly due to the presence of nonholonomic constraints. Choosing x_r^c not equal to $-d$, we may decouple and linearize the system.

Since $S^T E = I_{2\times 2}$, the nonlinear feedback, Equations (9) and (17), in this case is simplified to

$$\tau = (S^T M S)u + S^T M \dot{S}\nu + S^T V \quad (39)$$

and

$$u = \Phi^{-1}(q)(v - \dot{\Phi}(q)\nu) \quad (40)$$

The linearized and decoupled subsystems are

$$\ddot{y}_1 = v_1 \quad (41)$$
$$\ddot{y}_2 = v_2 \quad (42)$$

4 Motion Planning

For simplicity, a two link planar manipulator is considered in this discussion. Let θ_1 and θ_2 be the joint angles and L_1 and L_2 be the link length of the manipulator. Also let the coordinates of the manipulator base with respect to the platform frame X_c-Y_c be denoted by (x_b^c, y_b^c). We let the reference point to the end point of the manipulator at a preferred configuration. We choose the configuration that maximizes the manipulability measure of the manipulator. If we specify the position of the end point as the desired trajectory for the reference point, the mobile platform will move in such a way that the manipulator is brought into the preferred configuration. The manipulability measure is defined as [1]

$$w = \sqrt{\det(J(\theta)J^T(\theta))} \quad (43)$$

where θ and $J(\theta)$ denote the joint vector and Jacobian matrix of the manipulator. If we consider non-redundant manipulators, the equation (42) reduces to

$$w = |\det J(\theta)| \quad (44)$$

For the two-link manipulator shown in Figure 1, the manipulability measure w is

$$w = |\det J| = L_1 L_2 |\sin\theta_2| \quad (45)$$

Note that the manipulability measure is maximized for $\theta_2 = \pm 90°$ and arbitrary θ_1. We choose $\theta_2 = +90°$ and $\theta_1 = -45°$ to be the preferred configuration, denoting them by θ_{1r} and θ_{2r}. Then the coordinates of the reference point with respect to the platform frame X_c-Y_c is given by

$$x_r^c = x_b^c + L_1\cos\theta_{1r} + L_2\cos(\theta_{1r} + \theta_{2r}) \quad (46)$$
$$y_r^c = y_b^c + L_1\sin\theta_{1r} + L_2\sin(\theta_{1r} + \theta_{2r}) \quad (47)$$

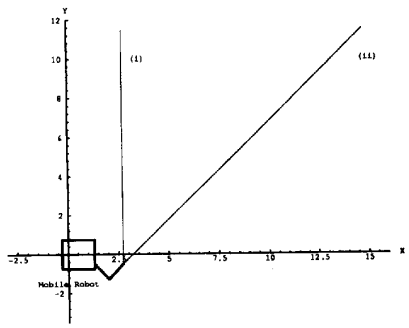

Figure 2: Two desired trajectories for simulations.

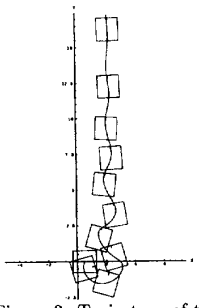

Figure 3: Trajectory of the point P_o for experiment (i)

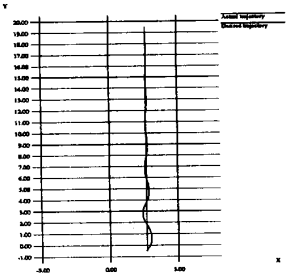

Figure 4: Desired and actual trajectories of the reference point for experiment (i)

We emphasize that x_r^c and y_r^c are constant and will be used in the representation of the output equation (33). The manipulator is regarded as a passive device whose dynamics is neglected. It is assumed that a human operator drags the end effector of the manipulator. The position of the end effector is given as the desired trajectory for the reference point P_r. The manipulator will be kept in the preferred configuration provided that the reference point is able to follow the desired trajectory. Any tracking error of the reference point will leave the manipulator out of the preferred configuation, resulting in a drop in manipulability measure. To count for measurement and communication delay, the current position of the end effector is made available to the mobile platform a fixed number of sampling periods later (five periods in the simulation). Further, before given to mobile platform as the desired trajectory, the position data of the end effector is approximated by piecewise polynomial functions generated in real time by *singular value decomposition*. This approximation is to eliminate high frequency (noise) components and to allow differentiation of discrete data in order to obtain desired velocity for the reference point.

5 Simulation

The mobile platform is initially directed toward positive X-axis at rest and the initial configuration of the manipulator is $\theta_1 = -45°$ and $\theta_2 = 90°$. Two different paths used for the simulation are shown in Figure 2. The velocity along the paths is constant.

1. A straight line perpendicular to the X-axis or the initial forward direction of the mobile platform,
2. A forward slanting line by 45 degree from X-axis.

The sampling rate is 0.01 sec. The linear state feedback gains for the two subsystems (41) and (42) are chosen so that the overall system has a natural frequency $\omega_n = 2.0$ and a damping ratio $\zeta = 1.2$. The higher damping ratio is to simulate the slow response of the mobile platform. For each simulation, we plot the trajectory of P_o, the trajectory of the reference point P_r, the manipulability measure, the joint angles of the manipulator, the heading angle of the platform, and the velocity of the P_o.

1. Figure 3 shows the trajectory of point P_o, in which a box[3] and a notch on one side represent the mobile platform and its forward direction, respectively. Note that the desired trajectory is

[3]These boxes are not equally distributed in time.

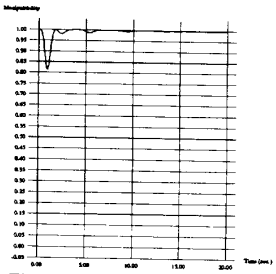

Figure 5: Manipulability measure for experiment (i)

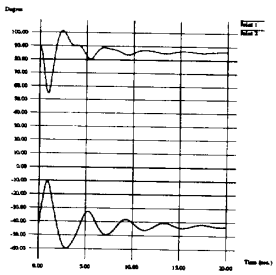

Figure 6: Joint angles for experiment (i)

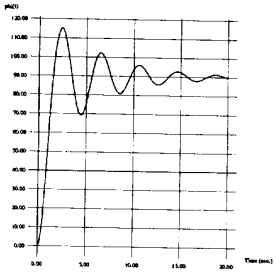

Figure 7: Heading angle for experiment (i)

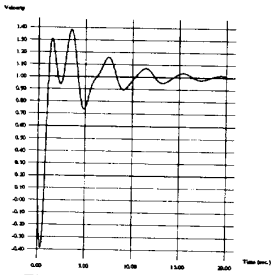

Figure 8: Velocity of the point P_o for experiment (i)

given for the reference point P_r. P_o has no desired trajectory. Figure 4 shows the desired and actual trajectories of the reference point P_r. The manipulability measure, the joint angles, the heading angle, and the velocity of point P_o are shown in Figure 5, 6, 7, and 8, respectively. Figure 5 shows a little degradation of manipulability measure corresponding to the early maneuver by the mobile platform. Figure 7 shows that the heading angle rapidly increases and exceeds 90° at the beginning, and evenually settles at 90°. The negtive value in Figure 8 indicates that the mobile platform moved backwards for a short period of time at the very beginning in order to achieve the needed heading angle. Note that the motion of the platform, or exactly the trajectory of point P_o is not planned. Therefore, the exhibited backward motion is not explicitly planned and is a consequence of the control algorithm.

2. The results for the slanting trajectory are shown in Figure 9 through 12. Figure 10 shows that the reference point follows the desired trajectory successfully. From Figure 11, the degradation of manipulability measure is smaller than that of the previous case as expected. Figure 12 indicates that that no backward motion occurs.

6 Experiment

The algorithm stated above is implemented with an experimental mobile manipulator. The system consists of a PUMA 250 6-DOF manipulator and a LABMATE platform (Figure 13). For simplicity only the first three joints of the manipulator are taken into account, *i.e.*, no wrist joints are considered. The sampling rates of PUMA 250 and

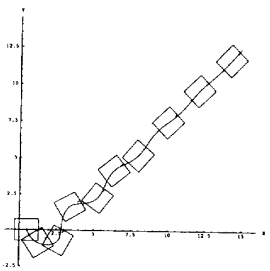

Figure 9: Trajectory of the point P_o for experiment (ii)

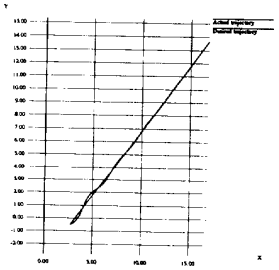

Figure 10: Desired and actual trajectries of the reference point for (ii)

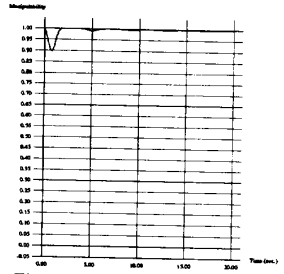

Figure 11: Manipulability measure for experiment (ii)

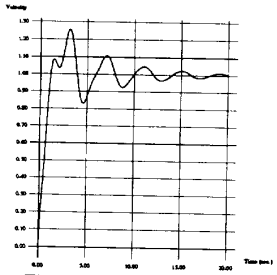

Figure 12: Velocity of the point P_o for experiment (ii)

Figure 13: Mobile manipulator used in the experiments.

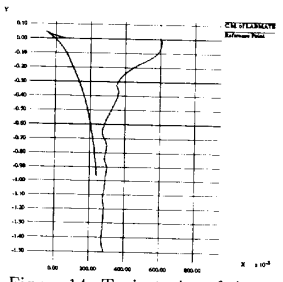

Figure 14: Trajectories of the P_o of LABMATE and the reference point

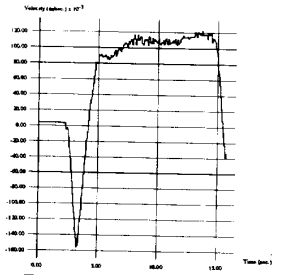

Figure 15: Velocity of the point P_o of LABMATE

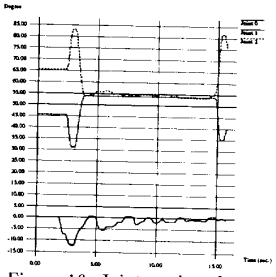

Figure 16: Joint angles of PUMA 250

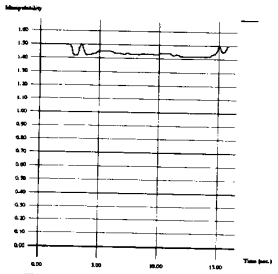

Figure 15: Manipulability measure

LABMATE are 250 and 16 Hz, respectively. In the experiment the end effector of the mobile manipulator which is at rest and in an optimal configuration in the beginning is dragged by a human operator. For comparison purpose it is dragged along the direction normal to the initial heading direction of LABMATE, which corresponds to the first trajectory in the simulations. Figure 14 shows the trajectories of the center of mass of LABMATE (P_o) and the reference point. The former trajectory indicates the platform initially goes backward and then starts moving forward. This observation agrees with the simulation result in the previous section though their transient behaviors are somewhat different. Figure 15 depicts the velocity of the center of mass of LABMATE, which also exhibits the presense of the initial backup. Note that dragging ceases at about 14 sec. Figure 16 shows the joint angles of the manipulator. The joints significantly change in the early stage, and then remain almost constant after the platform reaches an approximately constant velocity. Manipulability measure is shown in Figure 17. The manipulability slightly drops in the beginning and is maintained at the same level while the platform is in motion. It then comes back to a nearly optimal configuration after dragging stops. The slight degradation during motion is mainly due to the communication delay.

7 Concluding Remarks

We presented a planning and control algorithm for coordinating motion of a mobile manipulator. The design criterion was to control the mobile platform so that the manipulator is maintained at a configuration which maximizes the manipulability measure. We verified the effectiveness of our method by simulations on two representative trajectories. The algorithm was implemented with an actual mobile manipulator and tested on one of the trajectories for comparison purpose. For future work, we will investigate the integration of the proposed method and force control. An alternative path planning approach will be explored as mentioned in the previous section such that the maneuverability of mobile platform is taken into consideration as well.

Acknowlegement

This work is in part supported by NSF Grants CISE/CDA-90-2253, CISE/CDA 88-22719, and MSS-9157156, NATO Grant CRG 911041, Navy Grant N0014-88-K-0630, AFOSR Grants 88-0244 and 88-0296, Army/DAAL 03-89-C-0031PRI, and the University of Pennsylvania Research Foundation.

References

[1] Tsuneo Yoshikawa. *Foundations of Robtics: Analysis and Control.* The MIT Press, Cambridge, Massachusetts, 1990.

[2] J. Joshi and A. A. Desrochers. Modeling and control of a mobile robot subject to disturbances. In *Proceedings of 1986 International Conference on Robotics and Automation*, pages 1508–1513, San Francisco, CA, April 1986.

[3] G. J. Wiens. Effects of dynamic coupling in mobile robotic systems. In *Proceedings of SME Robotics Research World Conference*, pages 43–57, Gaithersburg, Maryland, May 1989.

[4] S. Dubowsky, P-Y. Gu, and J. F. Deck. The dynamic analysis of flexibility in mobile robotic manipulator systems. In *Proceedings of the Eighth World Congress on the Theory of Machines and Mechanisms*, page , Prague, Czechoslovakia, August 1991.

[5] N. A. M. Hootsmans. *The Motion Control of Manipulators on Mobile Vehicles.* PhD thesis, Department of Mechanical Engineering, Massachusetts Institute of Technology, Cambridge, Massachusetts, January 1992.

[6] Ju I. Neimark and N. A. Fufaev. *Dynamics of Nonholonomic Systems.* American Mathematical Society, Providence, RI, 1972.

[7] S. K. Saha and J. Angeles. Dynamics of nonholonomic mechanical systems using a natural orthoganal complement. *Transactions of the ASME, Journal of Applied Mechanics*, 58:238–243, March 1991.

[8] Anthony Bloch and N. H. McClamroch. Control of mechanical systems with classical nonholonomic constraints. In *Proceedings of 28th IEEE Conference on Decision and Control*, pages 201–205, Tampa, Florida, December 1989.

[9] J. Barraquand and Jean-Claude Latombe. On nonholonomic mobile robots and optimal maneuvering. In *Proceedings of Fourth IEEE International Symposium on Intelligent Control*, Albany, NY, September 1989.

[10] V. Kumar, X. Yun, E. Paljug, and N. Sarkar. Control of contact conditions for manipulation with multiple robotic systems. In *Proceedings of 1991 International Conference on Robotics and Automation*, Sacramento, CA, April 1991.

[11] Anthony Bloch, N. H. McClamroch, and M. Reyhanoglu. Controllability and stability properties of a nonholonomic control system. In *Proceedings of 29th IEEE Conference on Decision and Control*, pages 1312–1314, Honolulu, Hawaii, December 1990.

[12] G. Campion, B. d'Andrea-Novel, and G. Bastin. Controllability and state feedback stabilization of non holonomic mechanical systems. In C. Canudas de Wit, editor, *Lecture Notes in Control and Information Science*, pages 106–24, Springer-Verlag, 1991.

[13] J. P. Laumond. Finding collision-free smooth trajectories for a non-holonomic mobile robot. In *10th International Joint Conference on Artificial Intelligence*, pages 1120–1123, Milano, Italy, 1987.

[14] Z. Li and J. F. Canny. *Robot Motion Planning with Nonholonomic Constraints.* Technical Report Memo UCB/ERL M89/13, Electronics Research Laboratory, University of California, Berkeley, CA, February 1989.

[15] Jean-Claude Latombe. *Robot Motion Planning.* Kluwer Academic Publishers, Boston, MA, 1991.

[16] G. Lafferriere and H. Sussmann. Motion planning for controllable systems without drift. In *Proceedings of 1991 International Conference on Robotics and Automation*, pages 1148–1153, Sacramento, CA, April 1991.

[17] B. d'Andrea-Novel, G. Bastin, and G. Campion. Modelling and control of non holonomic wheeled mobile robots. In *Proceedings of 1991 International Conference on Robotics and Automation*, pages 1130–1135, Sacramento, CA, April 1991.

[18] C. Samson and K. Ait-Abderrahim. Feedback control of a nonholonomic wheeled cart in cartesian space. In *Proceedings of 1991 International Conference on Robotics and Automation*, pages 1136–1141, Sacramento, CA, April 1991.

[19] C. Canudas de Wit and R. Roskam. Path following of a 2-DOF wheeled mobile robot under path and input torque constraints. In *Proceedings of 1991 International Conference on Robotics and Automation*, pages 1142–1147, Sacramento, CA, April 1991.

[20] H. Nijmeijer and A. J. van der Schaft. *Nonlinear Dynamic Control Systems.* Springer-Verlag, New York, 1990.